UCRL-ID-108553

PCMDI
Program for Climate Model Diagnosis and Intercomparison

PCMDI Report No. 3

THE EFFECT OF HORIZONTAL RESOLUTION ON OCEAN SURFACE HEAT FLUXES IN THE ECMWF MODEL

by

Peter J. Gleckler and Karl E. Taylor

Program for Climate Model Diagnosis and Intercomparison
Lawrence Livermore National Laboratory, Livermore, CA, USA

August 1992

PROGRAM FOR CLIMATE MODEL DIAGNOSIS AND INTERCOMPARISON
UNIVERSITY OF CALIFORNIA, LAWRENCE LIVERMORE NATIONAL LABORATORY
LIVERMORE, CA 94550

ABSTRACT

Annual mean ocean surface energy fluxes have been studied as a function of horizontal resolution in the ECMWF model (cycle 33) and compared with Oberhuber's COADS (1959-1979) based empirical estimates. The model has been run at resolutions of T21, T42, T63 and T106 for 15 months with prescribed monthly varying climatological SST and sea ice. The T42 simulation was extended to 2 years, which enabled us to determine that many differences between the resolution runs were significant and could not be explained by the fact that individual realizations of an ensemble of years can be expected to give different estimates of the annual mean climate state. In addition to systematic differences between the modeled and the observed fluxes, the simulated fields of surface shortwave and longwave radiation showed much more spatial variability than the observed estimates. This may be attributable more to deficiencies in the observations than to errors in the model. The modeled latent and sensible heat fields were in better agreement with observations. The primary conclusion concerning the dependence of ocean surface fluxes on resolution is that the T21 simulation differed significantly from the higher resolution runs, especially in the tropics. Although the differences among the three higher resolution simulations were generally small over most of the world ocean, there were local areas with large differences. It appears, therefore, that in relation to ocean surface heat fluxes, a resolution greater than T42 may not be justified for climate model simulations, although the locally large differences found between the higher resolution runs suggest that convergence has not been achieved even at T106.

1. Introduction

Recent advances in computing technology have enabled investigators to intensify efforts to understand the effects of horizontal resolution on atmospheric general circulation models (AGCMs). The task of examining a model's dependence on horizontal resolution is a straightforward objective, but fully interpreting the findings remains an arduous challenge. Physical parameterizations used in AGCMs make use of scaling assumptions to relate processes resolved by models to those that are not. Such parameterizations can depend on horizontal resolution in nontrivial ways, making their relative sensitivities difficult to decipher. For instance, what causes the resolution dependence? How does one separate the sensitivity of two model variables that are known to depend on one another? To address such questions, it is necessary to identify all significant resolution dependencies in an AGCM in order to account for interacting feedbacks in the simulation. This report describes the effect of horizontal resolution on ocean surface energy fluxes in the European Centre for Medium Range Weather Forecasts (ECMWF) cycle 33 model.

To date, the resolution dependence of ocean surface energy fluxes has not been studied, although other features have been analyzed in detail. Kiehl and Williamson (1991), for example, have explained why the total cloud amount in the National Center for Atmospheric Research community climate model (CCM1) decreases dramatically with increasing model resolution. Using a similar version of the CCM1, Boville (1991) found that many dynamical aspects of the model improved as horizontal resolution was increased. In contrast, Boer and Lazare (1988), who addressed the issue of horizontal resolution with the Canadian Climate Centre (CCC) model, found a sensitivity to resolution, but no systematic improvement at higher resolutions. In short, different investigators have observed a variety of effects upon varying the horizontal resolution in AGCMs.

Despite the lack of unanimity, it has been suggested that there might be an optimal resolution for use in climate studies. The typical assessment of an optimal resolution is made by comparing the resolution dependent features of a simulation with the computational expense. Tibaldi et al. (1990) examined extended-range weather predictions with the ECMWF model and suggested that T21 might be too low for climate model simulations, but that T106 would be too costly. In this report,

the question of an optimal resolution for climate model studies will be revisited, but from the perspective of ocean surface energy fluxes.

Efforts to validate AGCM ocean surface fluxes have been limited because verification is restricted by the paucity of observations. The deficiencies of the bulk parameterizations also lead to uncertainties, and the problem is compounded because these parameterizations are used both in models and in empirical estimates. Weare (1989) presented a formulation to quantify the combined uncertainties in ocean surface energy fluxes resulting from the basic field measurements, the bulk parameterizations, and the deficiencies in spatial and temporal sampling. The technique was applied to Weare's tropical Pacific atlas (1981), yielding uncertainties in some areas as high as the mean fields themselves.

Randall et al. (1992) have compared the zonal mean features of land surface heat fluxes in 19 AGCMs. The study focused on model sensitivities by performing simulations with perturbations in the sea surface temperature (SST) of +2K and -2K with respect to control runs. The responses of the various AGCM surface energy fluxes are quite different, but appear to be closely linked to differences in the hydrological cycle. In general, this study found the response of the net surface energy flux was not dominated by cloud effects, but rather by changes in the latent heat flux.

In section 2 the experimental design will be outlined, along with a description of the observations used for model validation. The ocean surface fluxes of shortwave radiation (SW), longwave radiation (LW), latent heat (LH), sensible heat (SH) and net energy (N) will be examined as a function of horizontal resolution and compared to observations in sections 3-7. Discussion of the overall findings in this study are summarized in Section 8.

2. Experimental design

Four 15-month simulations have been performed with the ECMWF cycle 33 model (operational in 1989), each with a different horizontal resolution. The model utilizes the spectral transform method in the horizontal with triangular truncation in the spherical harmonic expansions. The horizontal resolution of the four runs are T21, T42, T63 and T106, corresponding to (longitude, latitude) grids of approximately (5.6°x5.6°), (2.8°x2.8°), (1.9°x1.9°) and (1.1°x1.1°) respectively. In each version there are 19 layers of unequal thickness, with finer resolution in the boundary layer. The T42 simulation was extended to 24 months so that two different simulated years at the same resolution could be compared to differences amongst the resolution runs. The model was forced with seasonally varying insolation. Sea surface temperatures and sea ice distributions varied daily by linear interpolation between climatological monthly mean values taken from Alexander and Mobley (1976). Each model run began with the same T106 January average initial conditions, although they are not identical because the T21, T42 and T63 runs required interpolation. The practical aspects of identifying resolution dependencies are clear. The relative computational expense of these resolution runs is approximately 1 : 4 : 15 : 76 respectively for T21, T42, T63 and T106. Further details concerning the version of the model and experimental design are described by Gates et al. (1992).

The objective of this report is to compare ocean surface energy fluxes obtained from simulations of varying resolution with each other and with observations. Due to the large observational uncertainties in these fields, the analyses will be limited large-scale features. The four components of the surface energy balance (SW, LW, LH, SH) and their sum (N) will be examined. The focus will be on annual mean fluxes, from which meridional heat transport in the ocean basins can be inferred. Annual means can be limiting because information regarding the amplitude of the seasonal cycle is lost, and thus two fields can appear similar for different reasons. Our research indicates, however, that seasonal variations do not invalidate the major conclusions to be drawn here.

There have been a number of observationally-based estimates of global ocean surface energy fluxes. An early estimate was made by Esbensen and Kushnir (1981), using the Comprehensive Ocean-Atmosphere Data Set (COADS). More recently, atlases were prepared by Hsuing (1985) based on data provided by the U.S. Naval

Fleet Numerical Oceanographic Center, and by Oberhuber (1988) making use of a 'quality-controlled' version of COADS. Oberhuber's dataset will be used here to compare with the ECMWF model resolution runs. The following fields are required to estimate observational surface energy fluxes with standard parameterization techniques: SST, sea level pressure, total cloud cover, 10m level wind speed, moisture and temperature. The COADS fields are compiled as monthly climatologies based on ship observations made between 1950 and 1979. Woodruff et al. (1987) suggested that these data are reliable estimates of 30-year means along common shipping routes and moderately reliable in other areas, but as previously mentioned the uncertainties are not well known.

The surface SW and LW radiative fluxes in AGCMs are a direct result of the computation of atmospheric radiative transfer, which for the ECMWF model is described by Morcrette (1991). The observational estimates of surface radiative fluxes, on the other hand, are obtained with simplified parameterization formulae (Oberhuber,1988). The surface fluxes of LH and SH are computed from the following bulk parameterizations in both the model and the observations:

$$LH = \rho L C_L v_s (q_s - q_g) \quad (1)$$

$$SH = \rho C_H v_s (\psi_s - \psi_g) \quad (2)$$

where ρ is the surface air density, L the latent heat of vaporization, v the wind speed, q the specific humidity, and C_L and C_H are the transfer coefficients for LH and SH respectively. The subscript 's' refers to surface air values (10m in the observations, and lowest model level for the model) whereas the subscript 'g' denotes ground or sea surface values in both the model and the observations. The diagnostic variable q_g is defined as the saturation specific humidity at the surface pressure and temperature. In the observational calculations ψ is the temperature (T), but in the model it is the dry static energy $c_pT + gZ$ (with c_p the heat capacity of dry air at STP). In the ECMWF model C_L and C_H are computed with the formulation of Louis (1979), and are equivalent over the ocean. For the observational estimates of the transfer coefficients, Oberhuber uses the Large and Pond (1982) parameterization. Both of these techniques of estimating the transfer coefficients are based on similarity theory and account for the effects of low level atmospheric stability.

In the following sections the structure of the discussion will be the same for each ocean surface energy flux field. The sequence of global maps will be: 1) observations, 2) the four resolution runs, 3) difference maps between resolution runs. In order to highlight the dependence of each field on resolution, the standard set of difference maps presented will be T21 - T42, T42 - T63, and T63 - T106. In each case the higher resolution is interpolated to the lower with a standard area-weighting technique in which the two grids are superimposed and for each grid cell a value is computed by averaging the contributions from the overlapping original grid cells weighted by the area defined by the intersection of the cells.

3. Surface net shortwave radiation and cloud cover

Plate 1a depicts Oberhuber's estimate of the annual-mean ocean surface net SW energy flux. As in all succeeding plots, fluxes into the ocean are defined as positive, and the gray regions represent land, sea ice or missing data. Measurements poleward of 40°S are insufficient for calculation of annual means except along the coast of South America. The estimate shown in Plate 1a suggests that the surface SW is fairly zonal in character. In Plate 1b-1e, the same field is shown for each of the model runs. At all resolutions, the model surface SW is systematically larger than the observations. This is clearly indicated in Fig. 1, where the zonal means are typically 40 W m^{-2} greater in the model than observed. Obvious differences in the spatial distribution of the observations and model runs are evident in Plate 1. Compared with the observations, the simulated SW is much less zonal in character, having large SW maxima in the eastern oceans at all model resolutions.

In general, the differences between the simulated and observed annual mean net SW are quite large, but it is difficult to distinguish between model flaws and observational inaccuracies. Weare's (1989) estimates of observational uncertainties in the tropical Pacific vary from 10 to 100 W m^{-2}, but outside the tropics uncertainties have not been fully quantified. Thus even though the difference between modeled and observed SW is discouragingly high (the RMS difference averaged over all oceans is 48-52 W m^{-2}, depending on resolution), criticism of the model's SW surface fluxes based on the observations is not warranted. It is not clear whether the surface insolation over the ocean in the annual mean is as zonally symmetric as observations suggest or as spatially inhomogenous as indicated by the model.

1 a

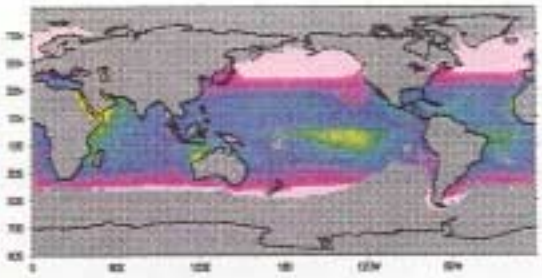

1 b

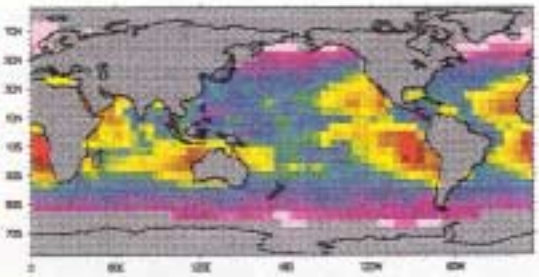

1 c

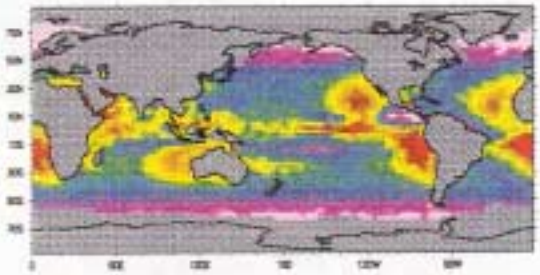

1 d

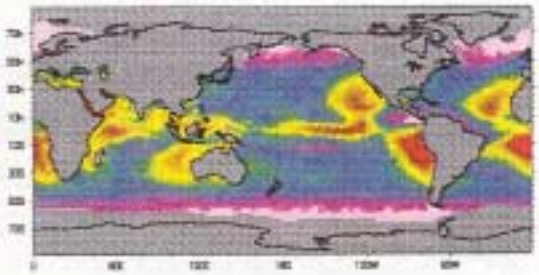

1 e

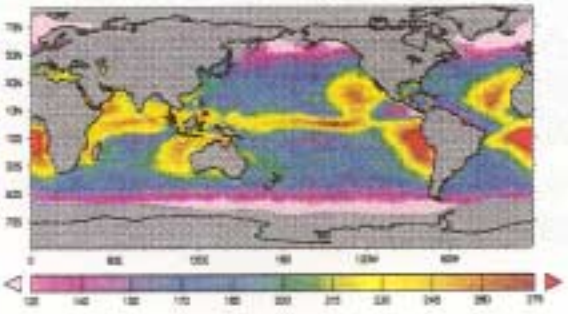

Plate 1. Annual mean net surface shortwave radiation (W m^{-2}).

a) Observations (Oberhuber)
b) T21
c) T42
d) T63
e) T106

2 a

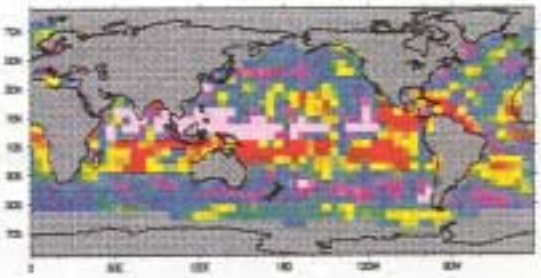

2 b

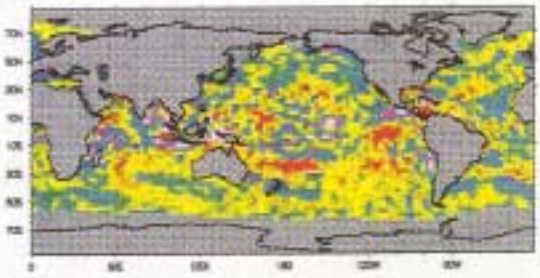

2 c

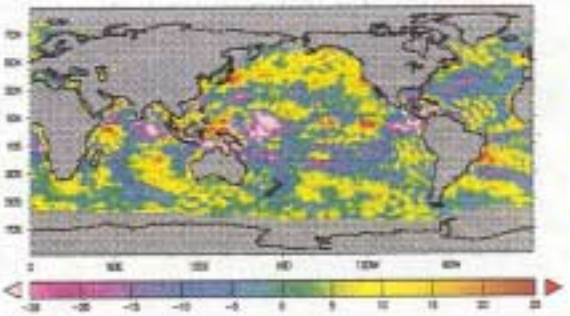

Plate 2. Difference maps of annual mean net surface shortwave radiation (W m^{-2}).

a) T21 - T42 (interpolated to T21)
b) T42 - T63 (interpolated to T42)
c) T63 - T106 (interpolated to T63)

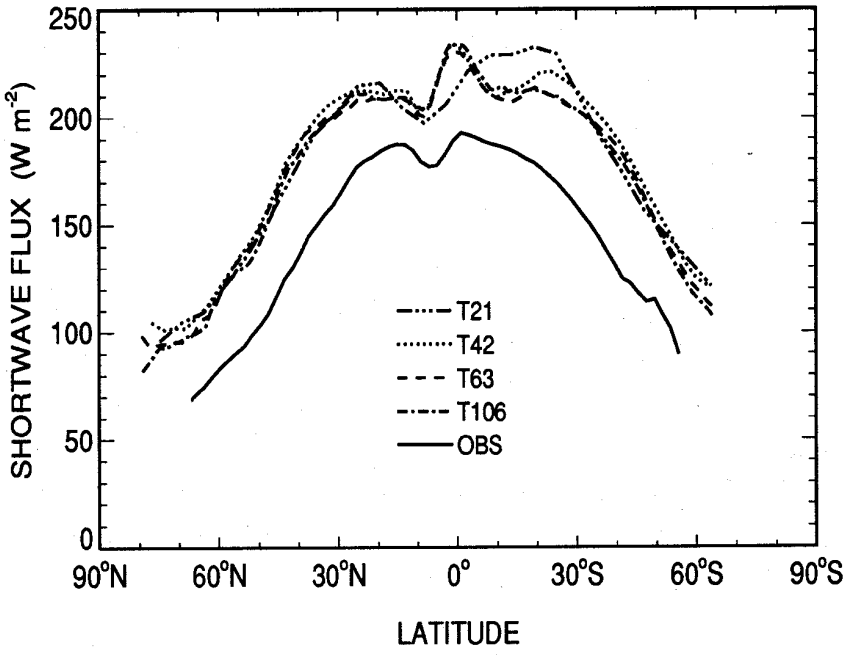

Fig. 1. Annual and zonal mean net surface shortwave energy flux in the ECMWF (cycle 33) AGCM and as estimated by Oberhuber using COADS.

Nor is it known which of the curves in Fig. 1 compares best with true climatology. In any case, Plates 1b-1e appear to show little difference between the SW in T42, T63 and T106. Many of the features of the T21 run resemble the higher resolution runs, but T21 does not have the distinct maximum SW in the equatorial Pacific seen at the higher resolutions, nor does it have the pronounced minimum just south of that region. There is a location just west of Panama with an extreme surface SW minimum at all resolutions except for T21. Reviewing Fig. 1, it is clear that the T21 simulation is distinctly different from the other model runs in the tropics, but at higher latitudes differences are not detectable in the zonal means.

The difference maps in Plate 2a-2c offer another perspective of the same information. While the similarities of the four simulations are clearly illustrated in Plates 1b-1e, Plates 2a-2c highlight the differences in the four resolutions. In Plate 2a the T21-T42 differences are shown to be at least $\pm$ 25 W m^{-2} throughout much of the tropical Pacific. The most prominent differences are due to the absence of the distinct tropical maximum and minimum in the T21 simulation. The differences between the

T42 and T63 simulations shown in Plate 2b are much smaller, with a range of 7 to 15 W m^{-2} over approximately 60% of the oceans, and a global ocean RMS difference of 12 Wm^{-2}. Likewise, the RMS difference corresponding to the T63 -T106 map in Plate 2c is 10.5 Wm^{-2}. Notice, however, that in both Plate 3b and Plate 3c there are isolated regions where differences are larger than $\pm$ 25 Wm^{-2}, though these areas are smaller in extent than in Plate 2a.

To determine whether model RMS differences of 10 Wm^{-2} are significant or can simply be attributed to internal atmospheric variability, ideally one should obtain an ensemble of realizations for each of the four different resolutions. In this study a less comprehensive statistical analysis is possible because only two realizations at only one of the resolutions (T42) were generated (the second realization being obtained by extending the integration through a second year with the same prescribed seasonally varying SST). Figure 2 shows the zonally averaged RMS difference in SW between the different resolutions and also the two realizations of the T42 run (designated year 1 and year 2). In tropical latitudes the differences between the models are much greater than the differences between the two years of the T42 simulation, whereas at middle and high latitudes this is not generally the case. This means that the surface SW over the oceans clearly depends on resolution in the tropics, but outside this region differences might be due to normal statistical fluctuations associated with an ensemble of annual cycle runs.

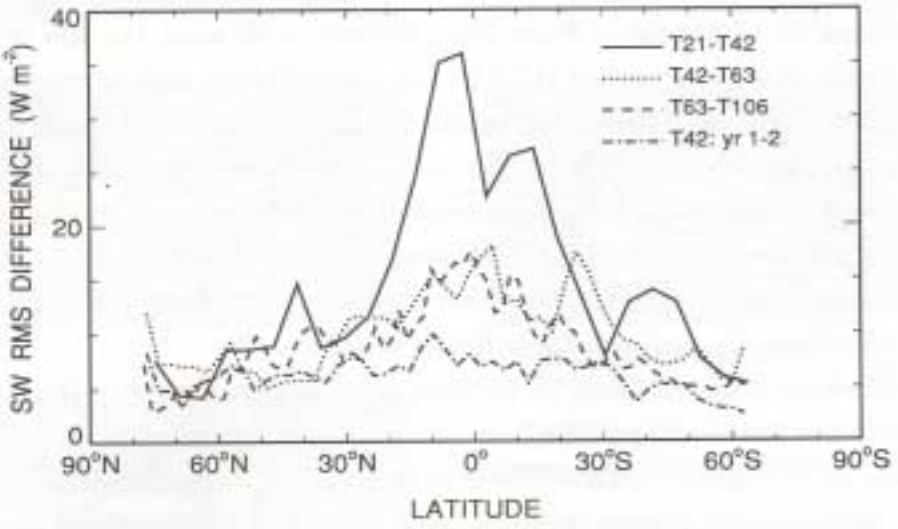

Fig. 2. Zonal average RMS differences of annual mean ocean surface shortwave radiation.

One interesting feature of Plates 2b and 2c is that in some locations these maps appear to be spatially anti-correlated in the sense that in regions of positive values in one map there are negative values in the other map. For example, the values >25 W m^{-2} in Plate 2b near 160E and 10N have changed to <-25 W m^{-2} in Plate 2c. Similar features can be observed just east of Panama and west of Sumatra. Changes as large but in the opposite sense can been seen in a small area near 150W and 5N. This suggests that in these regions at least, the model is not converging monotonically with increasing horizontal resolution. Overall, however, the differences between T106 and T63 are slightly smaller that the differences between T63 and T42, according to the calculated RMS differences given earlier.

The surface insolation is largely dictated by solar zenith angle and cloud cover. The daily and seasonal variations in solar zenith angle are clearly independent of model resolution, but clouds may not be. Plate 3a shows the annual mean cloud cover over the oceans according to the COADS (Wright, 1988) climatology compiled from ship observations. This is the data set used by Oberhuber to compute surface insolation and is therefore appropriate for understanding the observed SW shown in Fig. 1a. Satellites have provided a more uniform observational basis for creating cloud climatologies. Rossow et al. (1991), for example, have presented figures showing that the ISCCP cloud cover is systematically nearly 20% higher than the COADS climatology, yet the geographical distribution in the two are quite similar. Such differences indicate that significant observational uncertainty remains for this climatologically important field.

In Plates 3b-3e the annual mean cloud cover is shown for the resolution runs. As with the surface SW flux, the model cloud cover is qualitatively similar for the three higher resolutions, but distinctly different for the T21 run. The global means obtained from the model simulations and observations are similar (T21: 54%, T42: 48%, T63: 50%, T106: 51% and observations: 49%), but the cloud distributions in all the model runs are very different from the observations. A particular feature found at all resolutions is that there is little cloud cover off the west coast of every continent, a feature not seen in the COADS or ISCCP data. This helps to explain the excessive modeled surface SW flux seen in the eastern oceans in Plates 1b-1e.

The cloud cover difference maps for the resolution runs are shown in Plates 4a-4c. In some areas the differences seen here are more than 10%, despite the fact that the global means are within 3% of one another. To quantify the extent to which dif-

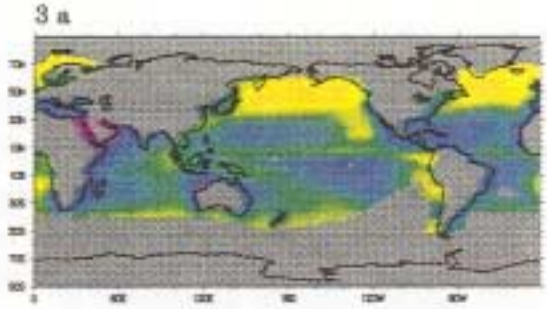

Plate 3. Annual mean cloud cover (percent).

a) Obeervations (Oberhuber)
b) T21
c) T42
d) T63
e) T106

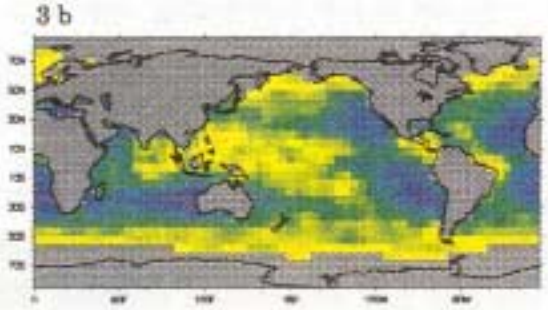

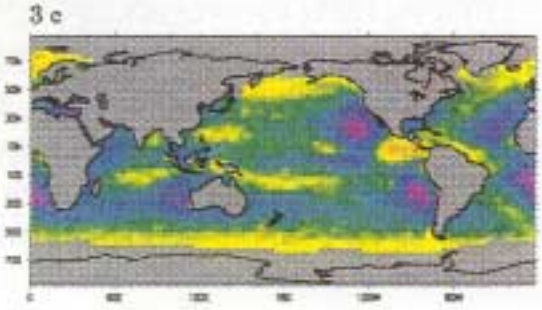

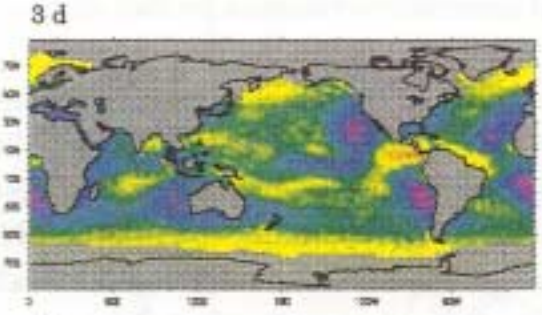

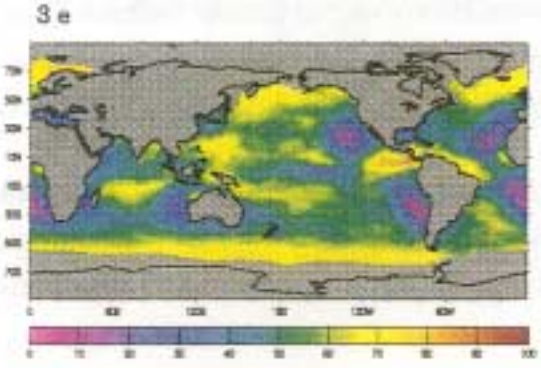

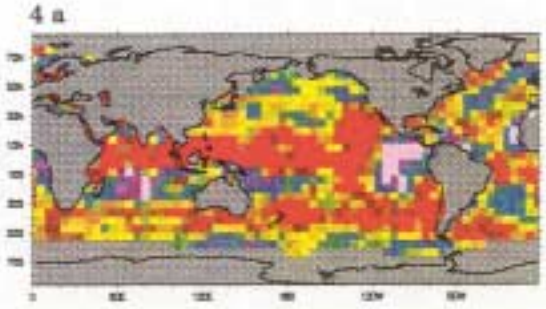

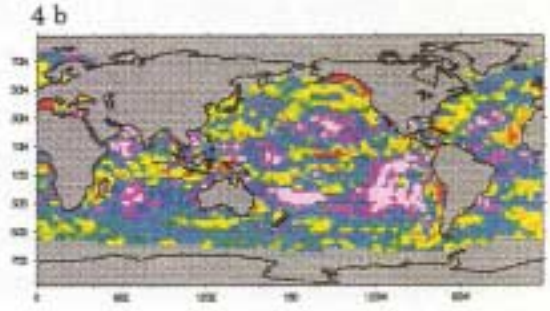

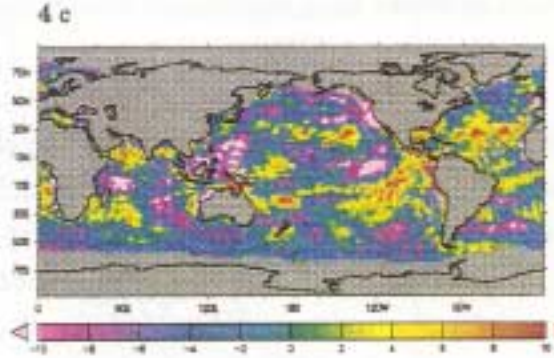

Plate 4. Difference maps of annual mean cloud cover (percent).

a) T21 - T42(interpolated to T21)
b) T42 - T63(interpolated to T42)
c) T63 - T106(interpolated to T63)

ferences in SW flux can be attributed to differences in cloud cover, we calculated the correlation coefficient between the SW difference fields shown in Plate 2 and the comparable differences in pairs of cloud cover fields shown in Plate 4. For the three pairs of resolution runs (T21-T42, T42-T63, and T63-T106), the correlation coefficients between surface SW and cloud cover were -0.77, -0.75, and -0.65, respectively. This means that about 50% of differences in the SW fields shown in Plate 2 may be explained by a linear dependence on annual average cloud cover differences shown in Plate 4. We suspect that had we accounted for the fact that nighttime cloud cover has no effect on SW and summertime cloud cover generally has a larger effect than winter-time cloud cover, we would have found an even higher correlation.

4. Surface net longwave radiation

The annual mean surface net LW radiation derived by Oberhuber is shown in Plate 5a. The scale was chosen to best display results from the resolution runs, and consequently much of the observed LW is off the low end of the scale. However, it is clear that the observed surface LW is spatially more homogeneous than the SW, shown in Plate 1a, and typically one third the magnitude. Over at least half of the observational domain the net LW is between -35 and -50 Wm^{-2} (net flux out of the ocean), and elsewhere values lie between -50 and -71 Wm^{-2}. In general the greatest surface net upward flux is in the subtropics, which is clearly related to the reduced cloud cover and moisture in regions of subsidence (e.g., the eastern Mediterranean, the Sea of Japan, and off the east and west coasts of Australia).

In Plates 5b-5e the LW field is shown for each of the resolution simulations. As was seen with the surface SW, comparison with the observations shows that the model's results have more spatial variability and systematically greater magnitudes at all resolutions. The difference between the zonally-averaged observed LW and simulated LW (not shown) is in the range of 10 to 30 W m^{-2}. The range of the surface LW for T42, T63 and T106 is from -25 W m^{-2} to -140 W m^{-2}, nearly three times the range of the observations. This higher spatial variability is due to differences along latitude circles. As shown in Fig. 3 the variance along latitude circles in the subtropics is an order of magnitude smaller in the observations than in any of the simulations. Again, however, the observations are so uncertain that we cannot be sure whether the net LW over the oceans is as spatially homogeneous as the observations, or is as highly variable as the model results.

5 a

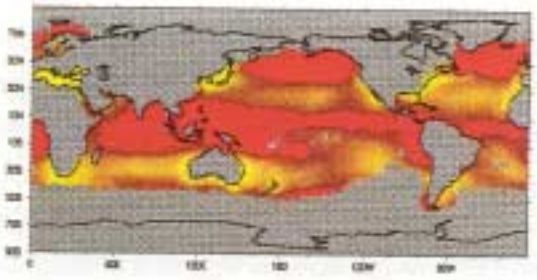

5 b

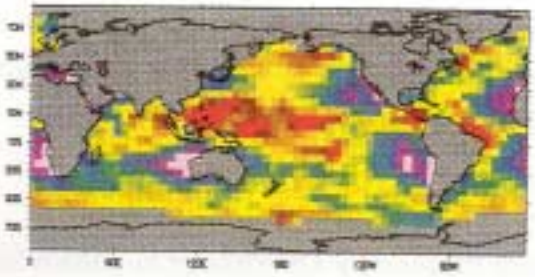

5 c

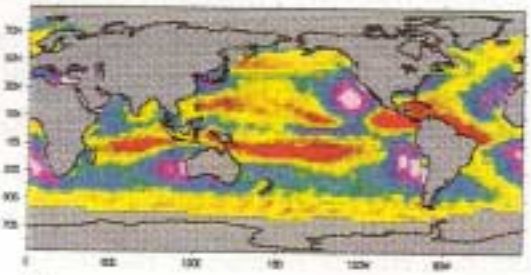

5 d

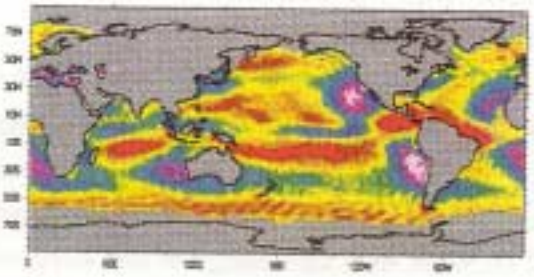

5 e

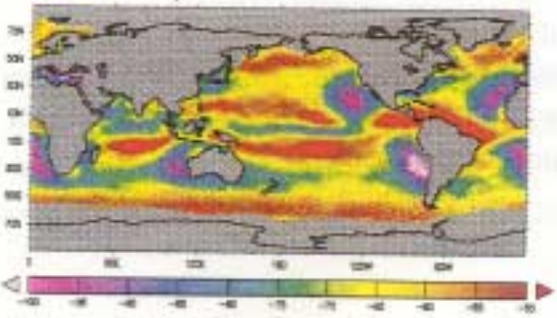

Plate 5. Annual mean net surface longwave radiation (W m^{-2}).

a) Observations (Oberhuber)
b) T21
c) T42
d) T63
e) T106

6 a

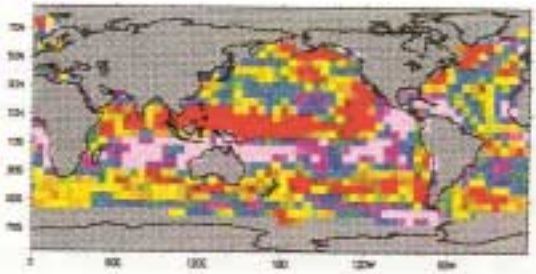

6 b

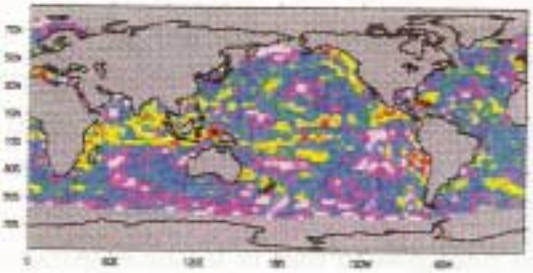

6 c

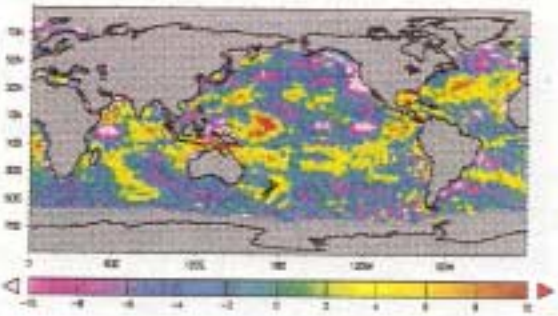

Plate 6. Difference maps of annual mean net longwave radiation (W m^{-2}).

a) T21 - T42 (interpolated to T21)
b) T42 - T63 (interpolated to T42)
c) T63 - T106 (interpolated to T63)

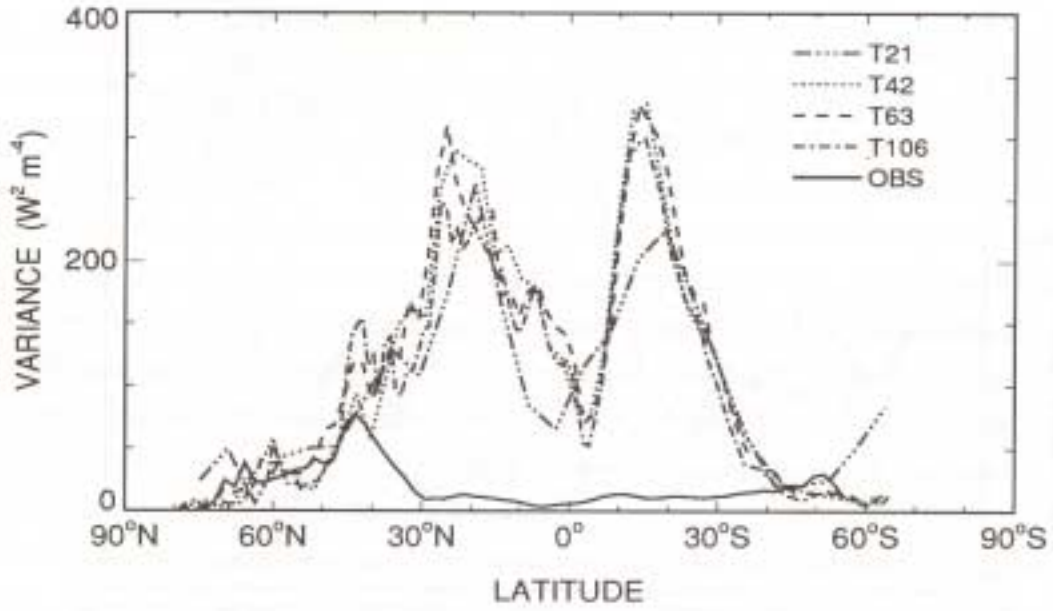

Fig. 3. Zonal average variance of annual mean ocean surface longwave radiation.

In contrast to the large differences between the observed and modeled LW, the results simulated at T42, T63 and T106 appear very similar. Overall, the gross features in the T21 simulation are similar to the higher resolution runs, but in some regions T21 appears to be quite different, such as in the Indian Ocean.

In Plates 6a-6c the longwave difference maps are shown. As in the SW, the T21-T42 map (Plate 6a) shows large differences, especially in the tropical Pacific. The pattern over the tropical Pacific in this map bears an obvious resemblance to the difference pattern for surface SW shown in Plate 2a. This suggests that a common cause is almost surely to be the differences in cloud cover between T21 and T42. More generally, the RMS differences in LW between the four resolution runs shown in Fig. 4 are quite similar to the RMS differences in SW shown in Fig. 2, but their magnitude is smaller by about a factor of two. For LW the differences seem to be significant even at high latitudes, and cannot be simply attributed to the statistical fluctuations to be expected from simulations with slightly different initial conditions. Most of the differences in the T42-T63 and T63-T106 maps are small (<10 Wm^{-2}), but as with the SW there are some exceptions. As suggested with the SW, the surface net

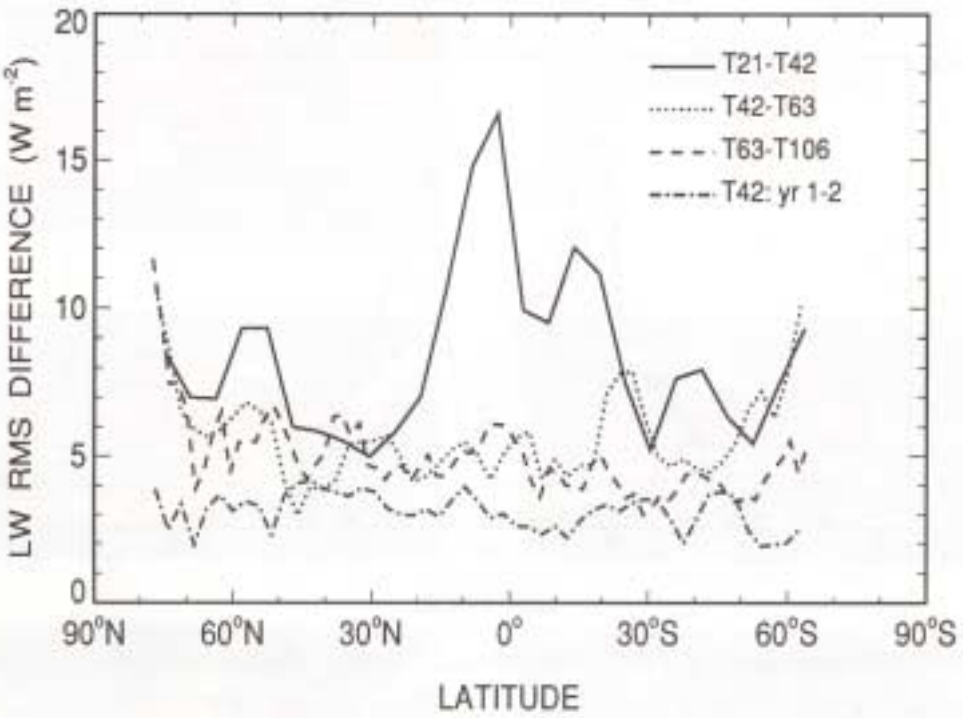

Fig. 4. Zonally averaged RMS difference of annual mean net surface longwave radiation.

LW field does not appear to be converging in a systematic way. Despite this, on the whole the differences are slightly smaller in the highest resolution difference pair (Plate 6c). The differences between the various resolutions in the surface net LW must be related to the differences in the distributions of clouds, temperature and water vapor. It is difficult to separate the effects of each of these, but it appears that total cloud cover may dominate. The spatial correlation between the annual mean cloud amount differences and the surface net LW differences for the T21-T42, T42-T63 and T63-T106 cases is 0.76, 0.67 and 0.67, respectively. It is possible that temporal correlations between the variations in cloud cover and net LW might explain some of the remaining differences, although differences in the vertical distribution of clouds might also be important.

5. Surface latent heat flux

The latent heat flux is the second largest component of the ocean surface energy budget. Oberhuber's estimate of LH is shown in Plate 7a. The observational uncertainties in LH, however, are thought to be the largest of the surface energy flux terms. In the tropical Pacific, Weare (1989) found the total uncertainty in LH to be at least 35 Wm^{-2}. An outstanding feature seen in Plate 7a is the intense evaporation observed over the Gulf Stream and Kuroshio currents where evaporation exceeds absorbed insolation. In both regions, the combination of dry continental air and warm SSTs intensifies the evaporation. The LH is also high in the subtropics, where subsidence minimizes low level atmospheric moisture which in turn stimulates evaporation. The LH is at a minimum along eastern oceanic boundaries and over the eastern tropical and northern Pacific oceans.

In Plate 7b-7e, the annual mean LH is shown for the four resolution runs. Model results at all resolutions are in much better agreement with the observations than was found for the SW and LW. This is intriguing when it is remembered that the uncertainties in the LH field are believed to be by far the largest uncertainties in the surface energy flux components. As was the case with the fields already examined, the T21 LH flux distribution is somewhat different from those at the higher resolutions. In the T21 simulation the effects of the Gulf Stream are not captured, but they are seen at the higher resolutions. There is also much less evaporation over the high latitude oceans at T21. Overall, the RMS difference between T21 and T42 is 24 $W\ m^{-2}$, more than twice the RMS differences between the higher resolution pairs. It is clear from Fig. 5 that in the tropical latitudes the differences between the resolution runs are larger than the year to year variability associated with the two year T42 simulation.

While the relatively low evaporation rate observed along the eastern ocean boundaries also appears in the model runs, in some areas of the subtropics, the evaporation greatly exceeds the observational estimates. A disturbing feature in the T42, T63 and T106 runs is the relatively large evaporation off the west coast of Panama. Anomalies in many other fields appear in this same region, for which no satisfactory explanation is in hand.

7 a

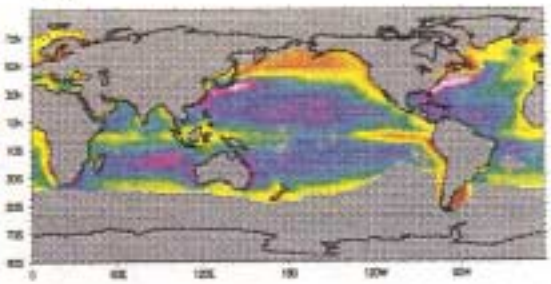

Plate 7. Annual mean latent heat flux (W m^{-2}).

a) Observations (Oberhuber)
b) T21
c) T42
d) T63
e) T106

7 b

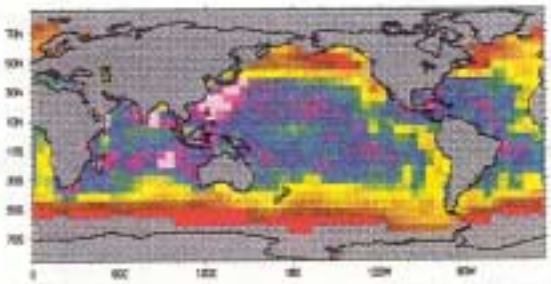

8 a

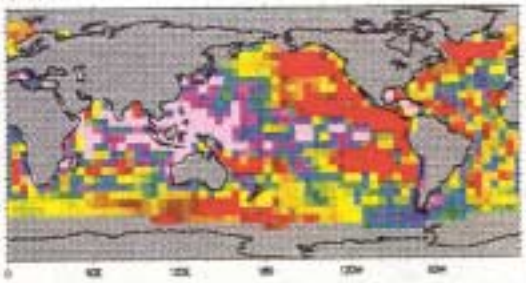

7 c

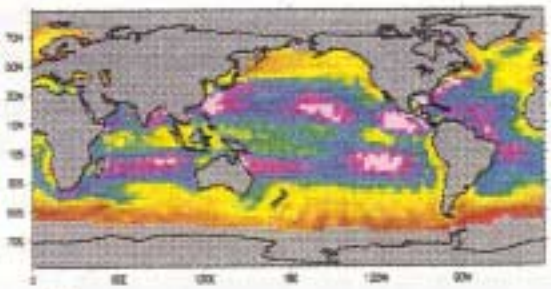

8 b

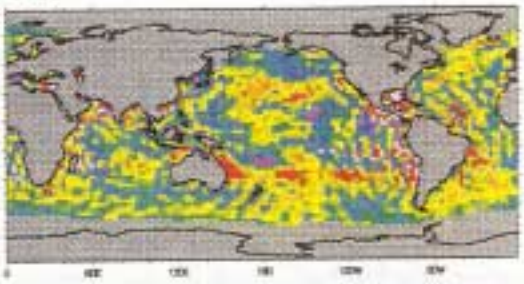

7 d

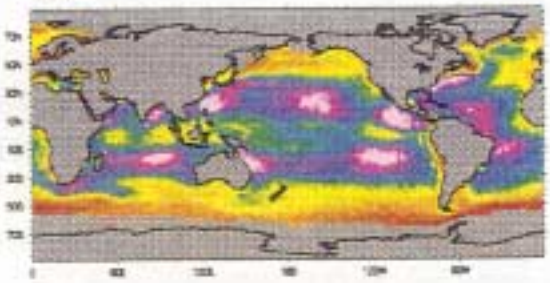

8 c

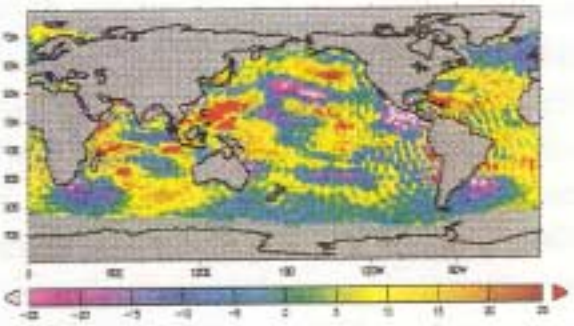

7 e

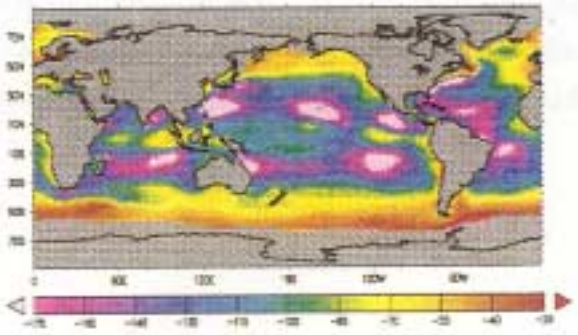

Plate 8. Difference maps of annual mean latent heat flux (W m^{-2}).

a) T21 - T42 (interpolated to T21)
b) T42 - T63 (interpolated to T42)
c) T63 - T106 (interpolated to T63)

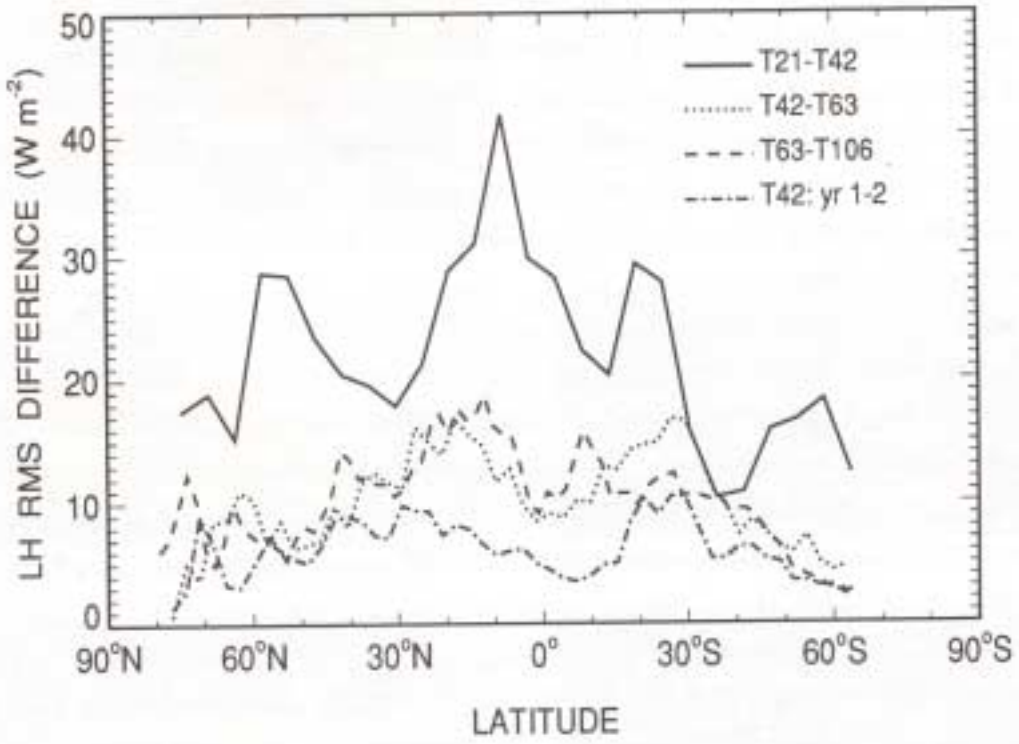

Fig. 5. Zonally averaged RMS difference of annual mean ocean surface latent heat flux.

In Plate 8a-c the resolution difference maps for LH are shown. As in the SW and LW fields the differences between T21 and T42 are generally the largest, but in this case the extreme differences are not found in the same areas as in the radiation fields. Inspection of the T42-T63 and T63-T106 differences in Plate 8 suggests that the evaporation is in general decreasing with resolution; this is confirmed by the global averages which for T21, T42, T63 and T106 are -69.5, -70.5, -67.9 and -66.9 Wm^{-2} respectively. There are some exceptions, however, such as off the west coast of Panama in the T63-T106 map (see Plate 8c). In summary, despite the uncertainties in the observations, the similarities of LH between the observations and the resolution runs are encouraging. As in the fields previously examined, significant local differences are found even at the two highest resolutions, indicating that at T106 convergence may not have been reached.

6. Surface sensible heat flux

The observational estimates of surface sensible heat flux are shown in Plate 9a. Over much of the ocean the SH flux is between 0 and -10 Wm^{-2}, making this the least important component of the ocean surface energy budget. The exceptions are over the Kuroshio and Gulf Stream currents, where the sensible heat loss of the oceans is generally above 30 Wm^{-2}. In the eastern equatorial Pacific, and in some coastal regions, the observations indicate that the oceans are gaining a small amount of sensible heat from the atmosphere.

In Plate 9b-9e, the annual mean SH is shown for the four resolution runs. At all resolutions the model SH flux in most areas is between 10 and 20 Wm^{-2},so that sensible heat loss of the oceans is generally greater than observations indicate. The SH flux over the western boundary currents is similar to the observations, but the fluxes are much smaller (more negative). The resolution run difference maps appear in Plate 10a-c. The relative differences in the T21-T42 map appear quite large, but compared to the other fields the differences in magnitude are small. In the two higher resolution maps the differences in many regions are near zero. There are a few regions where the relative differences in the T63-T106 difference map stand out, such as the southern Indian Ocean, and the northern Pacific and Atlantic Oceans. They are however, small in comparison to the magnitude of the differences seen in the SW and LH model fluxes. Many of the inferences made regarding the effect of resolution on LH also apply to the SH. It is again worth noting that the differences in the SH between one resolution and the next are substantially larger than the differences between the two T42 simulations. Unlike the SW, LW and LH fields, however, this is also true in most midlatitude regions for the SH , as seen in Fig. 6.

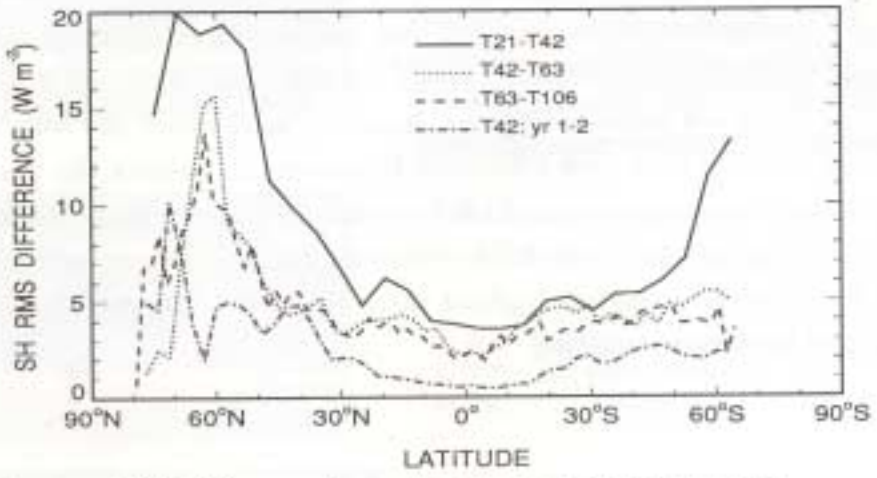

Fig. 6. Zonal average RMS differences of annual mean ocean sensible heat flux.

9 a

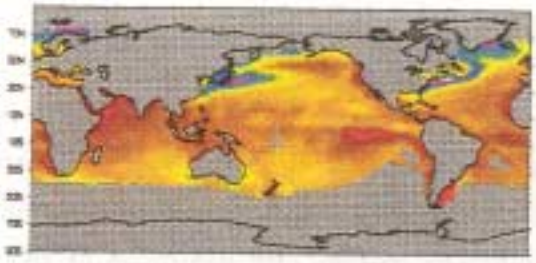

9 b

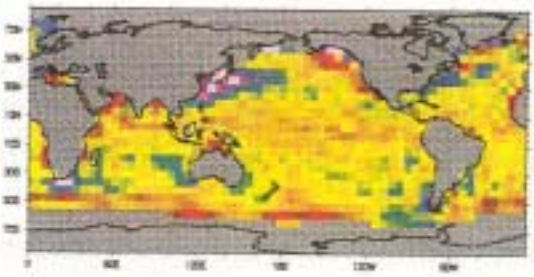

9 c

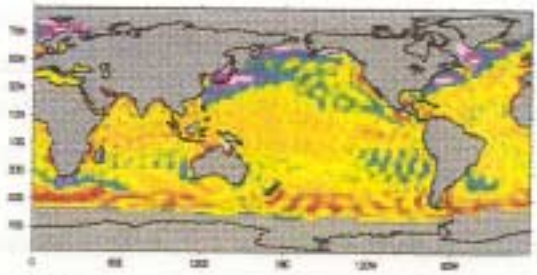

9 d

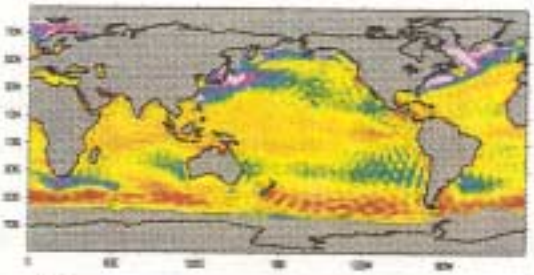

9 e

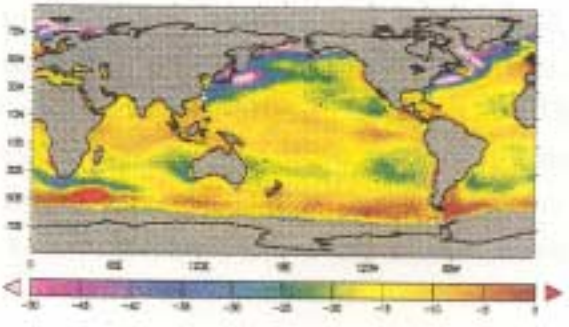

Plate 9. Annual mean sensible heat flux (W m^{-2}).

a) Observations (Oberhuber)
b) T21
c) T42
d) T63
e) T106

10 a

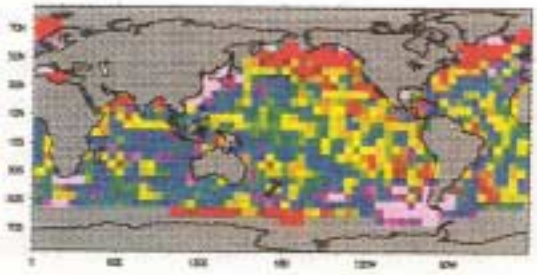

10 b

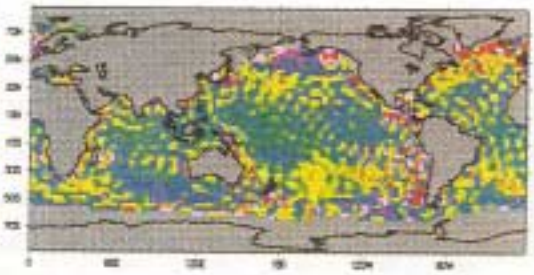

10 c

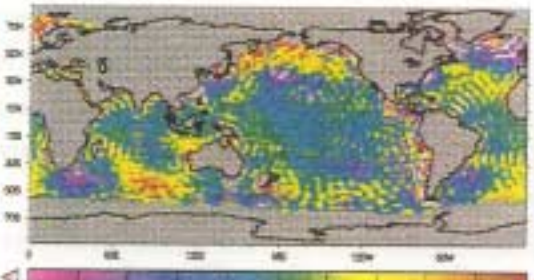

Plate 10. Difference maps of annual mean sensible heat flux (W m^{-2}).

a) T21 - T42 (interpolated to T21)
b) T42 - T63 (interpolated to T42)
c) T63 - T106 (interpolated to T63)

7. Net surface heat flux and implied meridional ocean heat transport

By adding the SW, LW, LH and SH fluxes together we obtain the surface net flux N. The N resulting from Oberhuber's flux fields are shown in Plate 11a. From a comparison of the magnitudes of the individual surface flux components, it is clear that the net flux is dominated by the SW and LH fluxes. The influence of LH is apparent in the intense evaporation over the western boundary currents, while the SW contribution is seen in the intense heating along the equatorial Pacific. Because of the relatively homogenous spatial pattern of the LW flux, it has little influence on the characteristics of the N distribution. For the land surface energy budget the SH flux is important, but with the exception of a few regions (most notably over the western boundary currents), its contribution to N is secondary.

In Plates 11b-e the annual mean N for the resolution runs are shown. As anticipated from examination of the individual flux fields, the T21 net flux is seen to be substantially different from the other resolutions. There is much less energy lost over the Gulf Stream than there is in the observations or the other resolution runs, and the structure over most of the Pacific Ocean is different. The higher resolution distributions of N are more similar to the observations, although there are a few regions of large discrepancies. The extreme cooling off the west coast of Panama is not seen in the observations, and in general the ocean cooling in the subtropical Pacific is much greater than observed. In the Bay of Bengal, the model runs indicate net cooling of the oceans whereas the observations suggest a warming.

The resolution difference maps for N are shown in Plates 12a-c. Here we see that there is little compensation between the surface flux components when resollution is varied. In fact, the differences shown in Plates 12a-c are larger than those of the fields that make up the net flux.

Imposing the SST as a lower boundary condition is a powerful constraint on an AGCM; it is, however, a useful simplification because the only direct effect the ocean has on the atmosphere is through the SST. Making use of the annual mean net surface energy flux, one can diagnose the heat transport required in the ocean in order to maintain the given spatial distribution of SST. A critical assumption is that there is no interannual variability in the distribution of oceanic heat content, but in general, the global annual mean ocean surface energy flux is not balanced in model simulations with prescribed SSTs. The annual mean imbalance for the resolution runs

11 a

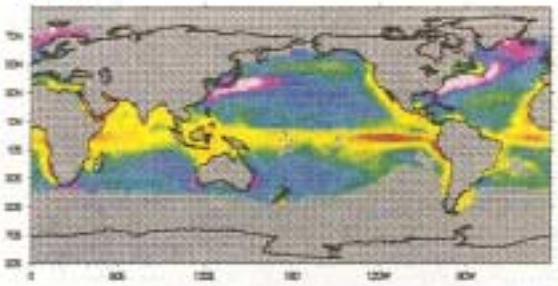

11 b

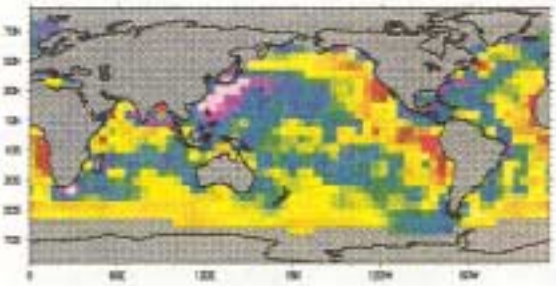

11 c

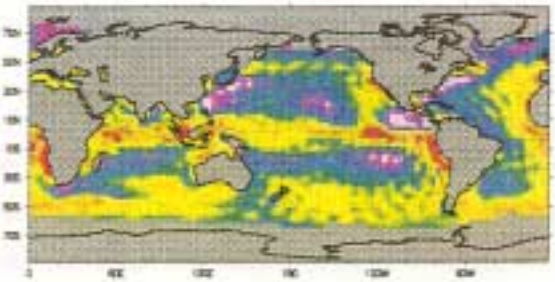

11 d

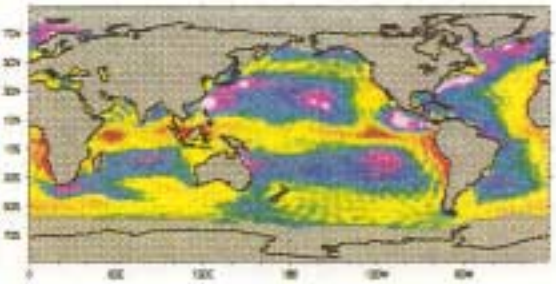

11 e

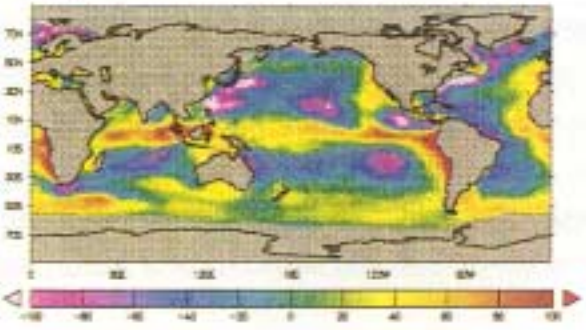

Plate 11. Annual mean net ocean surface heat flux (W m^{-2}).

a) Observations (Oberhuber)
b) T21
c) T42
d) T63
e) T106

12 a

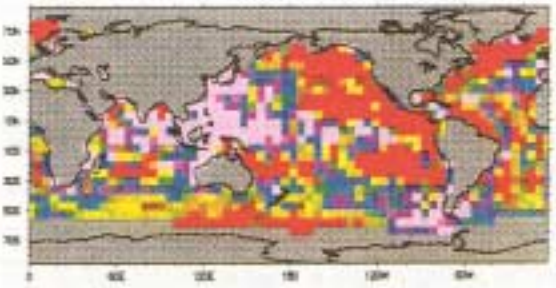

12 b

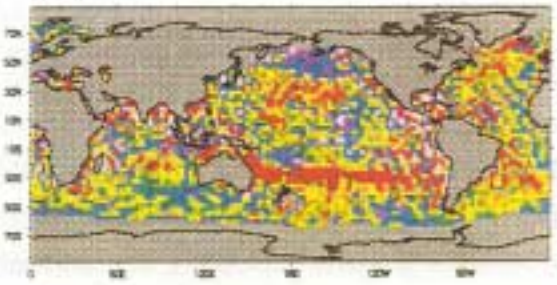

12 c

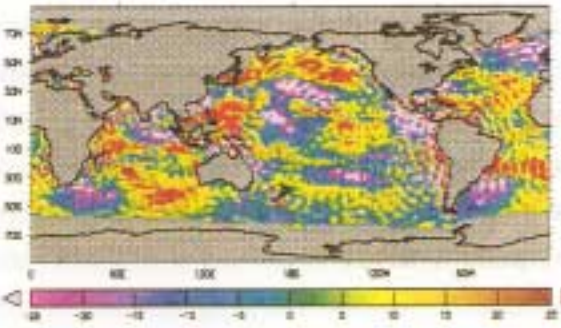

Plate 12. Difference maps of annual mean net ocean surface heat flux (W m^{-2}).

a) T21 - T42 (interpolated to T21)
b) T42 - T63 (interpolated to T42)
c) T63 - T106 (interpolated to T63)

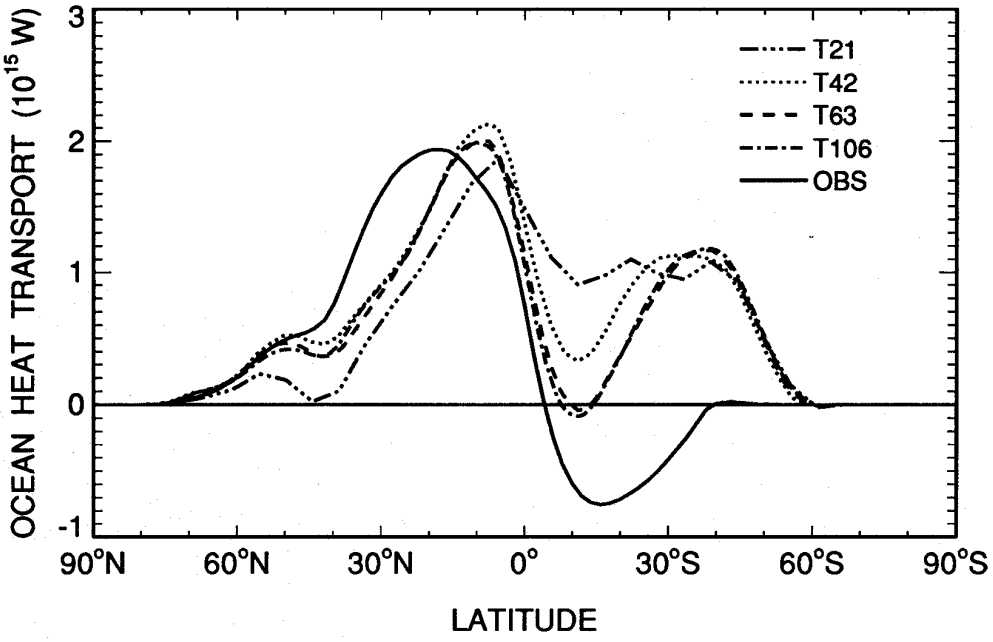

Fig. 7. Annual and zonal mean implied meridional oceanic poleward heat transport.

was 15.0, 10.9, 5.9 and 4.1 W m^{-2}, for T21, T42, T63 and T106, respectively. In our diagnostic calculation the excess energy is assumed to be uniformly diffused to the deep ocean. Figure 7 depicts the zonally averaged annual mean meridional heat transport implied for the resolution runs and as computed from Oberhuber's climatology. The curve representing the observations is similar to a variety of observational estimates (cf. Hsuing, 1986, and Carissimo, 1985), with poleward heat transport in both hemispheres. This is clearly not the case for any of the resolution runs with the ECMWF cycle 33 model, all of which produce an implied northward heat transport in both hemispheres although each shows a minimum northward transport near 10°N as do the observations. It is believed that this defect can be attributed to excess heating of the oceans in the 45°S to 55°S zone. Although further diagnosis is necessary, the apparent convergence of the T63 and T106 transport estimates should be noted.

8. Concluding remarks

Model validation has traditionally been carried out with the best observed fields available. However, as efforts to understand climate change have intensified, it has become increasingly evident that the deficiencies in our understanding of air - sea interactions, which are a stringent test on a model, may limit further progress. It is well recognized that as anthropogenic influences on climate increase, the rate of climate change will be mediated by exchange of energy between the atmosphere and ocean. Current uncertainties in observational ocean surface net energy flux estimates are at least an order of magnitude greater than the anticipated increase in LW radiative forcing resulting from a doubling of atmospheric carbon dioxide. Although it may not be necessary to reduce absolute errors to less that a few W m^{-2}, it will be essential to validate the ability of climate models to realistically simulate *changes* in surface energy fluxes of less than 1 W m^{-2}. Here we have taken a small step towards that goal by showing how in one climate model the surface fluxes depend on horizontal resolution.

Even with the present uncertainties in the observational data, we have been able to identify some consistent discrepancies between the ECMWF model simulations and observations. Chief among these is the ocean surface SW in the model (all resolutions), which is systematically nearly 40 Wm^{-2} greater than Oberhuber's estimates. This cannot be explained by the total cloud cover because the differences between the model and observed cloud fraction are not systematic. Moreover, it is not necessary for cloud fraction alone to account for all the differences since the surface SW depends on the cloud optical properties and indirectly on the vertical distribution of cloud cover (which largely determines the cloud liquid water content). Enhanced LW cooling, and to a lesser degree LH and SH, compensate for the model's larger SW.The model SW and LW fields contain much more spatial variability than is observed, but this is possibly due to the deficiencies in the ocean observations. The most obvious difference is that the surface SW is very high in the eastern oceans of all basins. This feature is also evident in the LW where the difference between the observed and modeled spatial variability is even more extreme. The spatial distribution of the simulated LH and SH compares much better to observations than the radiation fields. It is likely that this can be explained by the fact that the bulk parameterizations used in the model are similar to those used in the observational estimates, and because the SST to some extent dictates the range of flux values.

The most obvious general conclusion concerning the present resolution experiments is that for all of the fields examined there are significant differences between the T21 simulation and the higher resolution runs. The similarities between the T42, T63 and T106 simulations suggest that T42 may be sufficient for climate simulation studies with the ECMWF cycle 33 AGCM. Similar conclusions have been drawn by other investigators regarding this and other models. However, in general it does not appear that the model simulation has truly converged, even at T106. While the gross features of the simulation are largely invariant to resolution in the T42, T63 and T106 simulations, there are regions where the differences are large and thus could be important; the large changes are not systematic, as is evident when comparing the various difference maps of T42-T63 and T63-T106. These differences are believed to be significant, because they are much more pronounced than the differences between the first and second years of the T42 simulation.

In this study the parameterizations of the surface energy fluxes are identical for all resolutions. Thus the differences in fluxes must be due to differences in the fields that are used by the paramterizations. For the SW and LW fluxes we found, not surprisingly, that the changes in cloud from one resolution to another could explain a significant fraction of the differences in the radiation fields, but this conclusion is only the first step towards fully explaining our results. Ultimately one could presumably trace the causes for resolution dependence to the steeper horizontal gradients allowed by higher resolution, or to the horizontal advection and diffusion of the prognostic quantities in the model, which may also depend on model resolution. Given the large differences between the model results and observations, we think priority should be to given to validation of the model parametrizations and to reduction of the uncertainties in the observations.

Finally, a word of caution regarding the coupling of ocean and atmospheric models is in order. Although the basic features of the T42, T63 and T106 simulations seem to be similar, a closer look at the ocean surface energy balance has revealed that there are regions where there are significant differences between the resolution runs. It is conceivable that these differences in heating could have substantial influence on the ocean component of a coupled model. In short, these findings suggest that as coupled model simulations become more commonplace, it will be necessary to determine if the ocean model is sensitive to the horizontal resolution of the companion AGCM.

Acknowledgements: We thank W. L. Gates for providing many useful comments on a draft of this paper, and the PCMDI programming staff, without which this analysis would not have been possible. The cooperation of Jean-Jacques Morcrette and the ECMWF in making their forecast model available and in providing expert technical advice for this research is gratefully acknowledged. We also thank J. Oberhuber for supplying his atlas. This work was performed under the auspices of the Department of Energy Environmental Sciences Division by the Lawrence Livermore National Laboratory under contract W-7405-ENG-48.

REFERENCES

Alexander, R.C., and R.L. Mobley, 1976: Monthly averaged sea surface temperatures and ice pack limits on a 1° global grid. *Mon. Wea. Rev.*, **104**, 143-148.

Boer, G.J., and R. Laprise, 1984: Some results concerning the effect of horizontal resolution and gravity-wave drag on simulated climate. *J. Climate*, **1**, 789-806.

Boville, B.A., 1991: Sensitivity of simulated climate to model resolution. *J. Climate*, **4**, 469-485.

Carissimo, B.C., A.H. Oort and T.H. Vonder Haar, 1985: Estimating the meridional energy transports in the atmosphere and ocean. *J.Phys.Oceanogr.*, **15**,82-91.

Esbensen, S.K., and Y. Kushnir, 1981: The heat budget of the global ocean: An atlas based on estimates from surface marine observations; Climatic Research Institute Report No. 29, Oregon State Univ., Corvallis.

Gates, W.L., J.S. Boyle, L.C. Corsetti, C. Covey, P.J. Glecker, T.J. Phillips, G.L. Potter, K.R. Sperber, and K.E. Taylor, 1992: The effects of horizontal resolution on the mean seasonal climate simulated with the ECMWF model. In preparation.

Hsuing, J., 1985: Estimates of global oceanic meridional heat transport. *J. Phys. Oceanogr.*, **15**, 1405-1413.

Hsuing, J., 1986: Mean surface energy fluxes of the oceans. *J. Geophys.Res.*, **91**, 10585-10606.

Kiehl, J.T., and D.L. Williamson, 1991: Dependence of cloud amount on horizontal resolution in the National Center for Atmospheric Research community climate model. *J. Geophys. Res.*, **96**, 10955-10980.

Large, W.G., and S. Pond, 1982: Sensible and Latent Heat Flux Measurments over the Sea. *J. Phys. Oceanogr.*, **12**, 464-482.

Louis, J.-F., 1979: A parametric model of vertical eddy fluxes in the atmosphere. *Bound.-layer Meteorol.*, **17**, 187-202.

Miller, M. J., A. C. M. Beljaars and T. N. Palmer, 1992: The sensitivity of the ECMWF model to the parameterization of evaporation from the tropical oceans. *J. Clim.*, in press.

Morcrette, J.-J., 1991: Radiation and cloud radiative properties in the ECMWF operational weather forecast model. *J. Geophys. Res.*, **96**, 9121-9132.

Oberhuber, J.M., 1988: The budgets of heat, buoyancy and turbulent kinetic energy at the surface of the global ocean. Max-Plank-Institute for Meteorology Report Number 15, Hamburg.

Randall, D.A., R.D. Cess, J.P. Blanchet, G.J. Boer, D.A. Dazlich, A.D. Del Genio, M. Deque, V. Dymnikov, V. Galin, S.J. Ghan, A. A. Lacis, H. Le Treut, Z.-X. Li, X. Z. Liang, B.J. McAvaney, V.P. Meleshko, J.F.B. Mitchell, J.-J. Morcrette, G.L. Potter, L. Rikus, E. Roeckner, J.F.Royer, U. Schlese, D.A. Sheinin, J. Slingo, A.P. Sokolov, K.E. Taylor, W.M. Washington, R.T. Wetherald, I. Yagai, and M.-H. Zhang, 1992: Intercomparison and interpretation of surface energy fluxes in atmospheric general circulation models, *J. Geophys.Res.*, **97**, 3711-3725.

Rossow, W.B., and R.A. Schiffer, 1991: ISCCP Cloud data products. *Bull. Amer. Meteor. Soc.*, **72**, 1-19.

Simonot, J.Y., and H. Le Treut, 1987: Surface heat fluxes from a numerical weather prediction system. *Climate Dyn.*, **2**, 11-28.

Stone, P., and J.S. Risby, 1990: On the limitations of general circulation climate models. *Geophys.Res.Let.*, **17**, 2173-2176.

Tibaldi, S., T.N. Palmer, C. Brankovic and U. Cubasch, 1990: Extended-range predictions with ECMWF models: Influence of horizontal resolution on systematic error and forecast skill. *Quart. J.Roy.Meteor.Soc.*, **116**, 835-866.

Weare, B.C., 1989: Uncertainties in estimates of surface heat fluxes derived from marine reports over the tropical and subtropical oceans. *Tellus*, **41A**, 357-370.

Weare, B.C., P.T. Strub, and M.D. Samuel, 1981: Annual mean surface heat fluxes in the tropical Pacific Ocean. *J. Phys. Oceanogr.*, **11**, 705-717.

Woodruff, S.D., R.J. Slutz, R.L. Jenne and P.M. Steurer, 1987: A comprehensive ocean-amosphere data set. *Bull. Amer. Meteor. Soc.*, **68**, 1239-1250.

Wright, P.B., 1988: An atlas based on the 'COADS' data set: Fields of mean wind, cloudiness and humidity at the surface of the global ocean. Max-Plank-Institute for Meteorology Report Number 14, Hamburg.